Kinematic correlations in double J/Ψ production

Nikolay P. Zotov

(SINP, Lomonosov Moscow State University)

in collaboration with

S.P. Baranov (Lebedev Institute Physics, Moscow, Russia)
A.M. Snigirev (SINP, Lomonosov Moscow State University)
A. Szczurek, W. Schäfer (Institute of Nuclear Physics PAN, Cracow, Poland)

DESY 12-183, arXiv:1210.1806

O U T L I N E

1. Introduction
2. Theoretical framework
3. Numerical results
4. Conclusions

1. Introduction

In the last years the production of J/Ψ pairs has attracted a significant attention in the context of searches for double parton scattering processes. A number of discussions has been stimulated by the mesurement of the double J/Ψ production c.s. at the LHCb experiment at CERN

R. Aaij et al. (LHCb Collaboration), PL B 707 (2012) 52

Theoretical estimations show that the single (SPS) and double (DPS) parton scattering contributions are comparable in size:

A.V. Berezhnoy,A.K. Likhoded, A.V. Luchinsky, A.A. Novoselov, PR D 84 (2011) 094023.
C.-H. Kom, A. Kulesza, W.J. Stirling, PRL 107 (2011) 082002.
S.P. Baranov, A.M. Snigirev, N.Z., PL B 107 (2011) 116.
A.A. Novoselov, arXiv:1106.2184.

However to disentangle the SPS and DPS mechanisms one needs to clearly understand the production kinematics.

The goal of the present study is to carefully examine the J/Ψ pair production properties in the different kinematical domains paying attention to the different contributing processes.

One the SPS side we consider the leading-order $\mathcal{O}(\alpha_s^4)$ subprocess and subleading $\mathcal{O}(\alpha_s^6)$ contribution from one-gluon exchange and two-gluon exchange mechanisms.

2. Theoretical framework

SPS contributions

At the leading order, $\mathcal{O}(\alpha_s^4)$, the SPS subprocess $g + g \to J/\Psi + J/\Psi$ is represented by a set of 31 "box" diagrams (some examples displayed in Fig. 1).

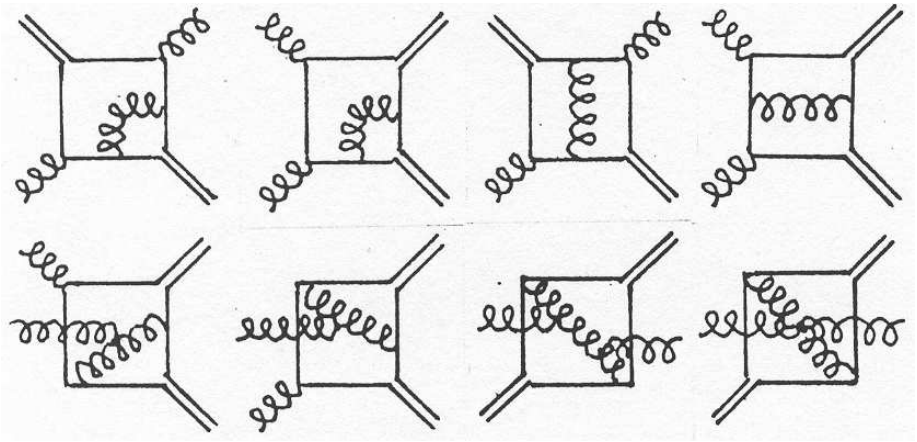

Figure 1: Examples of Feynman diagrams representing the leading-order gluon-gluon fusion subprocess $gg \to J/\Psi J/\Psi$.

Our approach is based on perturbative QCD, nonrelativistic bound state formalism and the k_T-factorization ansatz in the parton model.

The advantage of using the k_T-factorization approach comes from the ease of including the initial state radiation corrections that are efficiently taken into account in the form of the evolution of gluon densities. The calculation of this subprocess is identical to that described in

S.P. Baranov, PR D 84 (2011) 054012.

Only the color singlet channels are taken into consideration in the present study since this approach was found to be fully sufficient to describe all of the known LHC data on J/Ψ production:

S.P. Baranov, A.V. Lipatov, N.Z., PR D 85 (2012) 014034.

This process is also available in the hadron level Monte Carlo generator CASCADE**:**

H. Jung, S.P. Baranov,..., N.Z., EPJ C 70 (2010) 1237.

We also consider the pseudo-diffractive gluon-gluon scattering subprocesses represented by the diagrams of Fig. 2.
Despite the latter are of formally higher order in α_s, they contribute to the events with large rapidity difference between the two J/Ψ mesons and in that region can take over the leading-order 'box' subprocess. The pseudo-diffractive subprocesses are of our special interest as they potentially can mimic the DPS mechanism having very similar kinematics.

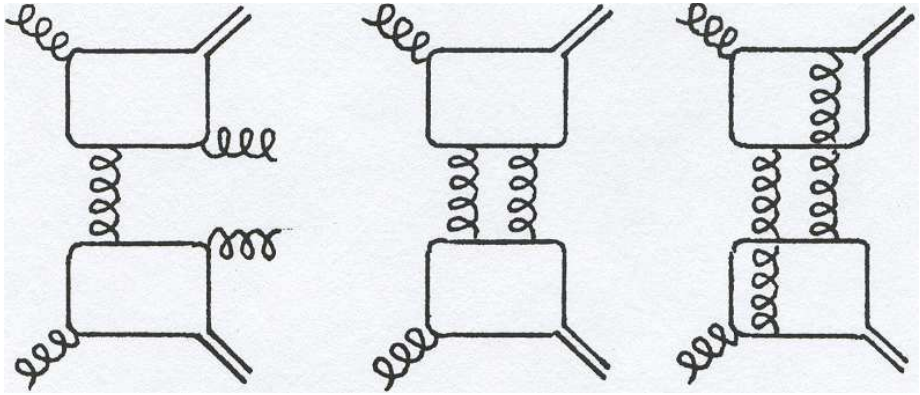

Figure 2: Examples of Feynman diagrams representing the production of J/Ψ pairs in pseudo-diffractive gluon-gluon scattering via one-gluon exchange and two-gluon exchange mechanisms.

The evaluation of the one-gluon exchange diagrams $g(k_1) + g(k_2) \to J/\Psi(p_1) + J/\Psi(p_2) + g(k_3) + g(k_4)$ is straightforward, but the number of diagrams is rather large. Note that the matrix element is free from infrared singularities. This is due to the specific property of the quark loop amplitude which vanishes when any of the three attached gluons becomes soft. These calculations have also been performed in the k_T-factorization.

The elementary $g + g \to J/\Psi + J/\Psi$ cross section can be calculated in the high-energy approximation similarly to how it was done for the $\gamma + \gamma \to J/\Psi + J/\Psi$ subprocess:

S.P. Baranov, A. Cisek, M. Kłusek-Gawenda, W. Schäfer, A. Szczurek, arXiv:1208.5917.

The corresponding cross section is proportional to $\alpha_s^6(\mu_r^2)$, and therefore depends strongly on the choice of the renormalization scale. In the calculation presented here we take $\mu_r^2 = m_T^2$ (m_T is the J/Ψ transverse mass).

The cross section for the two-gluon exchange contribution to the $p + p \to J/\Psi + J/\Psi + X$ reaction is calculated in the collinear approximation with MSTW 2008(NLO) gluon distribution function and the factorization scale $\mu_f^2 = m_T^2$.

We neglect the possible interference between the box diagram and the two-gluon exchange mechanism, which is formally of lower order than the square of the two-gluon amplitude. However, as it will become obvious from the numerical results, that the two-gluon mechanism is exceedingly small in the region of invariant masses dominated by the box mechanism.

DPS contributions

Under the hypothesis of having two independent hard partonic subprocesses A and B in a single pp collision, and under further assumption that the longitudinal and transverse components of generalized parton distributions factorize from each other, the inclusive DPS cross section reads

$$\sigma_{\rm DPS}^{\rm AB} = \frac{m}{2}\frac{\sigma_{\rm SPS}^{A}\sigma_{\rm SPS}^{B}}{\sigma_{\rm eff}}, \tag{1}$$

$$\sigma_{\rm eff} = \Big[\int d^2b\,(T(\mathbf{b}))^2\Big]^{-1}, \tag{2}$$

where $T(\mathbf{b}) = \int f(\mathbf{b_1})f(\mathbf{b_1}-\mathbf{b})\,d^2b_1$ is the overlap function that characterizes the transverse area occupied by the interacting partons, and $f(\mathbf{b})$ is supposed to be a universal function of the impact parameter b for all kinds of partons with its normalization fixed as

$$\int f(\mathbf{b_1})f(\mathbf{b_1}-\mathbf{b})\,d^2b_1\,d^2b = \int T(\mathbf{b})\,d^2b = 1. \tag{3}$$

The inclusive SPS cross sections $\sigma^A_{\rm SPS}$ and $\sigma^B_{\rm SPS}$ for the individual partonic subrocesses A and B can be calculated in a usual way using the single parton distribution functions.
Although these simplifying factorization assumptions are not sufficiently justified and are currently under revision, we restrict ourselves to this simple form (1) regarding it as the first estimate for the DPS contribution.

The presence of correlation term in the two-parton distributions results in reduction of the effective cross section $\sigma_{\rm eff}$ with the growth of the hard scale, while the dependence of $\sigma_{\rm eff}$ on the total energy at a fixed scale is rather weak. Thus, in fact, we obtain the lower bound estimate for the contribution under consideration. We used the value $\sigma_{\rm eff} \simeq 15$ mb in our analysis.

3. Results and discussion

We start with discussing the role of kinematic restrictions on the J/Ψ transverse momentum.

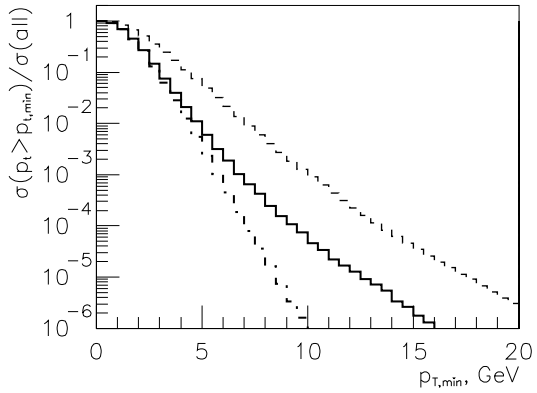

Figure 3: Fraction of the production cross section left after imposing cuts on the J/Ψ transverse momentum: Dashed line corresponds to requiring $p_T(\psi)>p_{T,min}$ for only one J/Ψ meson, dash-dotted line corresponds to the cuts on both J/Ψ's produced independently (DPS mode), solid curve - cuts on both J/Ψ's in real case (SPS mode).

On the contrary, in the naive the back-to-back kinematics, a cut applied to any of the two J/Ψ's would automatically mean the same restriction on the other, thus making no effect on the overall probability (dashed curve).

The solid curve (the explicit calculation) in the region $p_{T,min} < 4$ GeV coincides almost with the dash-dotted curve, thus showing that the two J/Ψ's are nearly idependent. With stronger cuts on $p_T(\psi)$, the curves diverge showing that the production of J/Ψ's becomes correlated.

Another illustration of this property is given by the distributions in the azimuthal angle difference $d\sigma(\psi\psi)/d\Delta\varphi$ exhibited in Fig. 4.

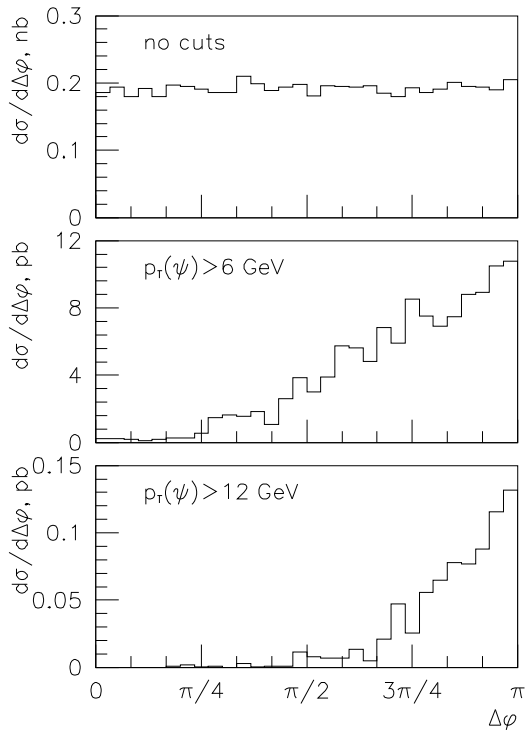

Figure 4: Azimuthal angle difference distributions after imposing cuts on the J/Ψ transverse momenta. Upper plot, no cuts; middle plot, $p_{T,min} = 6$ GeV; lower plot, $p_{T,min} = 12$ GeV. The distribution tends to concentrate around $\Delta\varphi \simeq \pi$ when the cuts on $p_T(\psi)$ become tighter.

In principle, one could get rid of the SPS contribution by imposing cuts like $p_T(\psi) > 6$ GeV, $\Delta\varphi < \pi/4$, but the DPS c.s. would then fall from tens of nanobarns to few picobarns.

We can conclude that the SPS and DPS modes are potentially distinguishable at sufficiently high $p_T(\psi)$, but the production rates fall dramatically, and so, the practical discrimination of the production mechanisms remains problematic.

We turn now to rapidity correlations explained in Figs. 5

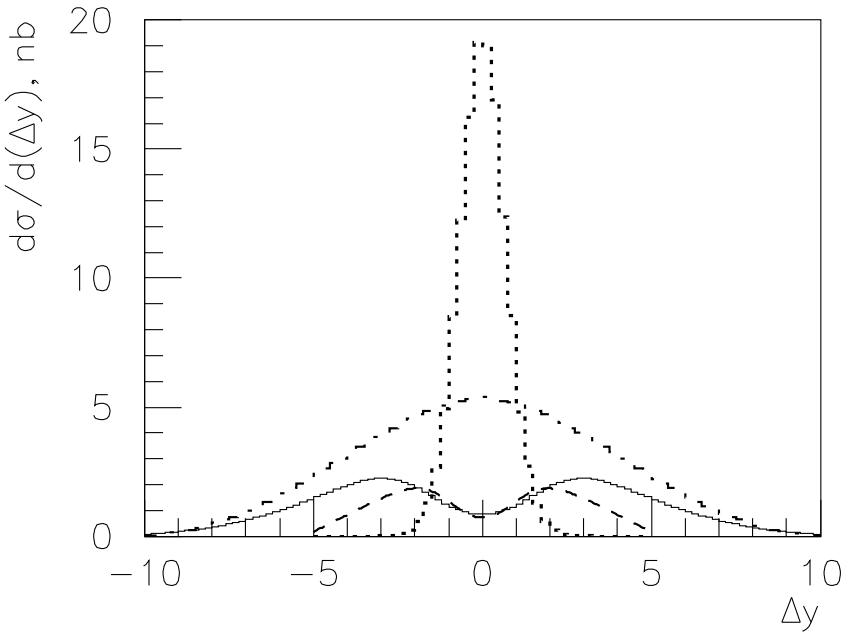

Figure 5: Distribution over the rapidity difference between J/Ψ mesons. Dotted curve, SPS 'box' contribution; the dash-dotted curve correspond to independent production (the DPS mode); dashed curve, one-gluon exchange contribution (multiplied by 1000); solid curve, two-gluon exchange contribution (multiplied by 25).

The absolute size of the one-gluon exchange cross section is found to be remarkably small.
The reasons of suppression of the one-gluon exchange cross section:

- **The presence of two extra powers of α_s.**
- **The large typical rapidity difference that makes the invariant mass of the final state relatively large: $M_{\psi\psi}(\Delta y{=}2)/M_{\psi\psi}(\Delta y{=}0) \simeq \cosh(\Delta y/2)$. Larger masses mean larger values of the probed x, and, accordingly, lower values of the gluon densities.**
- **The most important reason is in the color factors: 0.1 for the one-gluon exchange and -0.026 for the color interference term in comparison with 32/9 for the "box" diagram.**

The same suppression factors apply to the two-gluon exchange as well, but there is yet another suppressing mechanism specific for the one-gluon exchange process. It comes from the fact that the amplitude vanishes when any of the final state gluons becomes soft (this property makes the process infrared-safe).

3. Conclusions

- **We find it rather difficult to disentangle the SPS and DPS modes on the basis of azimuthal or transverse momentum correlations.**

  The difference becomes only visible at sufficiently high p_T, where the production rates are, indeed, very small.

- **Selecting large rapidity difference events looks more promising.**

  The leading order SPS contribution is localized inside the interval $|\Delta y| \leq 2$ (and continues to fall down steeply with increasing $|\Delta y|$), while the higher order contributions extending beyond these limits are heavily suppressed by the color algebra and do not constitute significant background for the DPS production.

Thank you for attention !